ORIGINAL PAPER

SOLITONS AND SHOCK WAVES SOLUTIONS FOR THE ROSENAU-KDV-RLW EQUATION

SEYDI BATTAL GAZI KARAKOC[1*], FUZHENG GAO[2], SAMIR KUMAR BHOWMIK[3]

Manuscript received: 27.07.2018; Accepted paper: 02.11.2018;
Published online: 30.12.2018.

Abstract. *In this article, a space time numerical scheme has been proposed to approximate solutions of the nonlinear Rosenau-Korteweg-de Vries-Regularized Long Wave (Rosenau-KdV-RLW) equation which represents the dynamics of shallow water waves. The scheme is based on a septic B-spline finite element method for the spatial approximation followed by a method of lines for the temporal integration. The proposed scheme has been illustarated with two test problems involving single solitary and shock waves. To demonstrate the competency of the present numerical algorithm the error norms* L_2 *,* L_∞ *and two lowest invariants* I_M *and* I_E *have been calculated. Linear stability analysis of the scheme has been studied using von-Neumann theory. The illustrated results confirm that the method is efficient and preserves desired accuracy.*

Keywords: *Rosenau-KdV-RLW equation, finite element method, collocation, septic B-spline, soliton.*

1. INTRODUCTION

The theory of shallow water waves is very important research field of theoretical, plasma and solid state physics, applied mathematics, fluid and water wave mechanics and nonlinear optics. Korteweg-de Vries (KdV),

$$U_t + aUU_x + bU_{xxx} = 0, \tag{0.1}$$

and Regularized Long Wave (RLW) equations,

$$U_t + U_x + aUU_x - bU_{xxt} = 0, \tag{0.2}$$

are two important mathematical models to define the dynamics of shallow water waves. RLW equation was created by Peregrine especially to describe the behavior of the undular bore [1]. Many physical phenomena, for example propagation of long waves in shallow water waves, bubble-liquid mixtures, ion acoustic plasma waves and wave phenomena in enharmonic

[1]* Department of Mathematics, Faculty of Science and Art, Nevsehir Haci Bektas Veli University, Nevsehir, 50300, Turkey. Corresponding Athor E-mail: sbgk44@gmail.com
[2] School of Mathematics, Shandong University, Shanda Nanlu, Jinan, Shandong, P. R.China. E-mail: fzgao@sdu.edu.cn
[3] Department of Mathematics, University of Dhaka, 1000 Dhaka, Bangladesh E-mail: bhowmiksk@gmail.com

crystals can be described by the KdV equation [2]. However KdV equation has a number of shortcomings. For example, it defines an unidirectional propagation of waves. Therefore, it can not describe the wave-wave and wave-wall interactions. Secondly, it was obtained under the presumption of weak anharmonicity so formation and the accomplishment of the high amplitude waves can not be well estimated by the KdV equation [3]. To overcome the shortcomings of the Eq. (1.1) , the following equation

$$U_t + U_x + U_{xxxxt} + \left(U^2\right)_x = 0, \tag{0.3}$$

was introduced by Rosenau [4, 5]. M. A. Park proved existence and uniqueness and certainty of the solutions of the Rosenau equation [6]. In order to make more detail studies on nonlinear waves the viscous term U_{xxx} was added to Eq. (1.3). Thus the updated mathematical model is

$$U_t + U_x + U_{xxx} + U_{xxxxt} + \left(U^2\right)_x = 0 \tag{0.4}$$

which is popularly known as Rosenau-KdV (R-KdV) equation. Numerical solutions of the R-KdV equation have been acquired by various methods. Zuo used the sine-cosine and the tanh methods for solving the R-KdV [7]. A conservative three-level linear finite difference scheme for the numerical solution of the initial-boundary value problem of R-KdV equation is suggested by J. Hu et al. [8]. The topological soliton solution or shock wave solutions of this equation was examined by G. Ebadi et al. [9]. The 1-soliton solution is obtained by the ansatz method for solitary waves and singular solitons and the soliton perturbation theory is implemented in order to define the adiabatic dynamics of the perturbed soliton by Razborova et al. [10]. In [11, 12], authors solved the equation with subdomain finite element method based on the sextic B-spline basis functions and septic B-spline collocation finite element method, respectively. At the same time, to discover different nonlinear behaviour of the waves, $-U_{xxt}$ has been used in Eq. (1.3) which is

$$U_t + U_x - U_{xxt} + U_{xxxxt} + \left(U^2\right)_x = 0. \tag{0.5}$$

This PDE is known as Rosenau-RLW (R-RLW). The numerical solutions of the R-RLW equation have been analyzed in recent years. Pan and Zhang [13] have considered the initial-boundary problem of the usual R-RLW equation by finite difference scheme and devising a protective numerical algorithm preserving the original conservative properties for the equation. Pan et al. [14] have developed the numerical solutions of the R-RLW equation using Crank-Nicolson type finite difference method and showed the existence of numerical solutions by Brouwer fixed point theorem. A new conservative difference scheme is analyzed by Zuo et al. [15]. The boundedness and convergence of the approximate solution for the semidiscrete Galerkin method to the R-RLW equation have been examined by Atouani and Omrani [16]. Also, a Galerkin finite element method is applied to R-RLW equation using cubic B-spline base functions by Yagmurlu et al. [17]. A mathematical form to get the solution of the nonlinear wave by coupling the Rosenau-KdV and the Rosenau-RLW equation has suggested by Wongsaijai and Poochinapan [18].

The Eqs. (1.4) and (1.5) can be combined which is popularly known as the following Rosenau-KdV-RLW equation with a power law nonlinearity:

$$U_t + aU_x - \gamma^{RLW} U_{xxt} + \beta^{KdV} U_{xxx} + bU_{xxxxt} + \alpha\left(U^n\right)_x = 0, \tag{0.6}$$

with the boundary conditions

$$U(a,t) = U(b,t) = 0, \quad U_x(a,t) = U_x(b,t) = 0, \quad U_{xx}(a,t) = U_{xx}(b,t) = 0, \quad t > 0, \tag{0.7}$$

and an initial condition

$$U(x,0) = f(x), \quad a \le x \le b. \tag{0.8}$$

In equation (1.6), the first term represents linear evolution while the parameter of a is advection or drifting term. γ and β are dispersion terms. The higher order dispersion and the parameter of nonlinearity terms are represented by b and α . If the parameter β^{KdV} and γ^{RLW} are taken zero, Eq. (1.6) turns into R-RLW and R-KdV equations, respectively. Razborova et al. [19,20] studied the dynamics of perturbed soliton solutions to the R-KdV-RLW equation with power law nonlinearity and computed the conservation laws of the R-KdV-RLW equation with power law nonlinearity by the aid of multiplier approach in Lie symmetry analysis. Also, the equation has been solved with ansatz method and semi-inverse variational principle by Razborova et al. [21]. Based on the multi-symplectic Hamiltonian formula of the generalized Rosenau-type equation, a multi-symplectic scheme and an energy-preserving scheme and local structure-preserving algorithms including multi-symplectic, local energy- and momentum-preserving schemes are introduced for the generalized Rosenau-RLW-KdV equation by Cai et al. [22,23]. The equation is considered with power nonlinearity by Ak et al. [24]. The dynamics of the one-dimensional, generalized KdV-RLW-Rosenau equation with second and fourth order dissipative terms subject to homogeneous boundary conditions and initial Gaussian conditions have been examined numerically by Fernandez and Ramos [25]. A three level linear conservative implicit finite difference algorithm for solving the R-KdV-RLW equation has been presented by Wang and Dai [26].

In this work, we focus on improving an efficient high accurate numerical method for Eq. (1.6) . To the best of our knowledge a higher order piecewise polynomial scheme for the space approximation of Eq. (1.6) has not been proposed and implemented before. Thus we aim to approximate the nonlinear PDE by higher order B-splines for the spatial approximation of Eq. (1.6) . To be specific we have designed a septic B-spline collocation method for the R-KdV-RLW equation followed by a method of lines for the time integration of the semi-discrete version of Eq. (1.6) . Numerical stability plays an important role to establish a numerical scheme. Here we also study the numerical stability of the scheme and analyze the numerical accuracy of the scheme briefly. We illustrate the scheme with some test examples. The rest of the article is organized in the following way:

-A collocation finite element method for the spatial approximation followed by a method of lines for the temporal integration of R-KdV-RLW equation has been proposed in Section 2. Resulting system can be solved with a variant of the Thomas algorithm.

- A linear stability analysis of the algorithm is examined in Section 3.
- A convergence of full discrete scheme has been discussed shortly in Section 4.
- In Section 5, motion of single solitary and shock waves have been analyzed with different initial and boundary conditions. Here we compare our results with that of some of those procurable in the literature.
- We finish with a short discussion and conclusion in Section 6.

2. COLLOCATION METHOD WITH SEPTIC B-SPLINES

We firstly choose the solution area of the problem limited over an region $a \le x \le b$. After this, we divided space region $[a,b]$ into equally sized finite elements of length h at the points x_m like that $a = x_0 < x_1 < ... < x_N = b$ and $h = \frac{b-a}{N}$. The septic B-spline functions $\phi_m(x)$ $(m = -3,-2,...,N+2,N+3)$ at the nodes x_m which form a basis for functions, described on the solution region $[a,b]$ by Prenter [27]

$$\varphi_m(x) = \frac{1}{h^7}\begin{cases} (x-x_{m-4})^7 & [x_{m-4}, x_{m-3}] \\ (x-x_{m-4})^7 - 8(x-x_{m-3})^7 & [x_{m-3}, x_{m-2}] \\ (x-x_{m-4})^7 - 8(x-x_{m-3})^7 + 28(x-x_{m-2})^7 & [x_{m-2}, x_{m-1}] \\ (x-x_{m-4})^7 - 8(x-x_{m-3})^7 + 28(x-x_{m-2})^7 - 56(x-x_{m-1})^7 & [x_{m-1}, x_m] \\ (x_{m+4}-x)^7 - 8(x_{m+3}-x)^7 + 28(x_{m+2}-x)^7 - 56(x_{m+1}-x)^7 & [x_m, x_{m+1}] \\ (x_{m+4}-x)^7 - 8(x_{m+3}-x)^7 + 28(x_{m+2}-x)^7 & [x_{m+1}, x_{m+2}] \\ (x_{m+4}-x)^7 - 8(x_{m+3}-x)^7 & [x_{m+2}, x_{m+3}] \\ (x_{m+4}-x)^7 & [x_{m+3}, x_{m+4}] \\ 0 & \textit{otherwise.} \end{cases} \tag{2.1}$$

Approximate solution $U_N(x,t)$ is stated in terms of the septic B-splines as

$$U_N(x,t) = \sum_{m=-3}^{N+3} \varphi_m(x)\delta_m(t) \tag{2.2}$$

where $\delta_m(t)$ are time dependent coefficients. Each septic B-spline covers eight elements, so each element $[x_m, x_{m+1}]$ is covered by eight B-splines. A spesific finite interval $[x_m, x_{m+1}]$ is planned to the region [0,1] by a local coordinate transformation identified by $h\xi = x - x_m$, $0 \le \xi \le 1$. Hence septic B-splines (2.1) in terms of ξ over [0,1] are given as follows:

$$\begin{aligned} \varphi_{m-3} &= 1-7\xi+21\xi^2-35\xi^3+35\xi^4-21\xi^5+7\xi^6-\xi^7, \\ \varphi_{m-2} &= 120-392\xi+504\xi^2-280\xi^3+84\xi^5-42\xi^6+7\xi^7, \\ \varphi_{m-1} &= 1191-1715\xi+315\xi^2+665\xi^3-315\xi^4-105\xi^5+105\xi^6-21\xi^7, \\ \varphi_m &= 2416-1680\xi+560\xi^4-140\xi^6+35\xi^7, \\ \varphi_{m+1} &= 1191+1715\xi+315\xi^2-665\xi^3-315\xi^4+105\xi^5+105\xi^6-35\xi^7, \\ \varphi_{m+2} &= 120+392\xi+504\xi^2+280\xi^3-84\xi^5-42\xi^6+21\xi^7, \\ \varphi_{m+3} &= 1+7\xi+21\xi^2+35\xi^3+35\xi^4+21\xi^5+7\xi^6-\xi^7, \\ \varphi_{m+4} &= \xi^7. \end{aligned} \tag{2.3}$$

For our scheme, the finite elements are defined with the region $[x_m, x_{m+1}]$. Using Eq. (2.1) and Eq.(2.2), the nodal values of $U_m, U_m^{'}, U_m^{''}, U_m^{'''}$ and U_m^{iv} are given in terms of the element parameters δ_m by

$$\begin{aligned}
&U_N(x_m,t) = U_m = \delta_{m-3} + 120\delta_{m-2} + 1191\delta_{m-1} + 2416\delta_m + 1191\delta_{m+1} + 120\delta_{m+2} + \delta_{m+3},\\
&U_m^{'} = \tfrac{7}{h}(-\delta_{m-3} - 56\delta_{m-2} - 245\delta_{m-1} + 245\delta_{m+1} + 56\delta_{m+2} + \delta_{m+3}),\\
&U_m^{''} = \tfrac{42}{h^2}(\delta_{m-3} + 24\delta_{m-2} + 15\delta_{m-1} - 80\delta_m + 15\delta_{m+1} + 24\delta_{m+2} + \delta_{m+3}),\\
&U_m^{'''} = \tfrac{210}{h^3}(-\delta_{m-3} - 8\delta_{m-2} + 19\delta_{m-1} - 19\delta_{m+1} + 8\delta_{m+2} + \delta_{m+3}),\\
&U_m^{iv} = \tfrac{840}{h^4}(\delta_{m-3} - 9\delta_{m-1} + 16\delta_m - 9\delta_{m+1} + \delta_{m+3})
\end{aligned} \tag{2.4}$$

and the variation of U over the element $[x_m,\ x_{m+1}]$ is shown by

$$U = \sum_{m=-3}^{N+3} \varphi_m \delta_m. \tag{2.5}$$

Substituting the approximate solution (2.2) and putting the nodal values of (2.5) and its derivatives given by (2.4) into Eq.(1.6) yields the following set of ordinary differential equations of the form

$$\begin{aligned}
&\dot{\delta}_{m-3} + 120\dot{\delta}_{m-2} + 1191\dot{\delta}_{m-1} + 2416\dot{\delta}_m + 1191\dot{\delta}_{m+1} + 120\dot{\delta}_{m+2} + \dot{\delta}_{m+3}\\
&+ \tfrac{7}{h}(-\delta_{m-3} - 56\delta_{m-2} - 245\delta_{m-1} + 245\delta_{m+1} + 56\delta_{m+2} + \delta_{m+3})\\
&- \tfrac{42}{h^2}(\dot{\delta}_{m-3} + 24\dot{\delta}_{m-2} + 15\dot{\delta}_{m-1} - 80\dot{\delta}_m + 15\dot{\delta}_{m+1} + 24\dot{\delta}_{m+2} + \dot{\delta}_{m+3})\\
&+ \tfrac{210}{h^3}(-\delta_{m-3} - 8\delta_{m-2} + 19\delta_{m-1} - 19\delta_{m+1} + 8\delta_{m+2} + \delta_{m+3})\\
&+ \tfrac{840}{h^4}(\dot{\delta}_{m-3} - 9\dot{\delta}_{m-1} + 16\dot{\delta}_m - 9\dot{\delta}_{m+1} + \dot{\delta}_{m+3})\\
&+ p\tfrac{7}{h}Z_m(-\delta_{m-3} - 56\delta_{m-2} - 245\delta_{m-1} + 245\delta_{m+1} + 56\delta_{m+2} + \delta_{m+3}) = 0,
\end{aligned} \tag{2.6}$$

where $Z_m = U_m = \delta_{m-3} + 120\delta_{m-2} + 1191\delta_{m-1} + 2416\delta_m + 1191\delta_{m+1} + 120\delta_{m+2} + \delta_{m+3})^{p-1}$.

If time parameters δ_i and its time derivatives $\dot{\delta}_i$ in Eq.(2.6) are decoupled by the Crank-Nicolson form

$$\delta_i = \frac{\delta_i^{n+1} + \delta_i^n}{2}, \tag{2.7}$$

and routine finite difference approach

$$\dot{\delta}_i = \frac{\delta_i^{n+1} - \delta_i^n}{\Delta t} \tag{2.8}$$

we derive a repetition connection between two time levels n and $n+1$ depending two unknown parameters δ_i^{n+1}, δ_i^n for $i = m-3, m-2, ..., m+2, m+3$

$$\gamma_1\delta_{m-3}^{n+1}+\gamma_2\delta_{m-2}^{n+1}+\gamma_3\delta_{m-1}^{n+1}+\gamma_4\delta_m^{n+1}+\gamma_5\delta_{m+1}^{n+1}+\gamma_6\delta_{m+2}^{n+1}+\gamma_7\delta_{m+3}^{n+1}$$
$$=\gamma_7\delta_{m-3}^{n}+\gamma_6\delta_{m-2}^{n}+\gamma_5\delta_{m-1}^{n}+\gamma_4\delta_m^{n}+\gamma_3\delta_{m+1}^{n}+\gamma_2\delta_{m+2}^{n}+\gamma_1\delta_{m+3}^{n}, \quad (2.9)$$

where

$$\begin{aligned}
&\gamma_1=[1-E(1+pZ_m)-M-K+T],\\
&\gamma_2=[120-56E(1+pZ_m)-24M-8K],\\
&\gamma_3=[1191-245E(1+pZ_m)-15M+19K-9T],\\
&\gamma_4=[2416+80M+16T],\\
&\gamma_5=[1191+245E(1+pZ_m)-15M-19K-9T],\\
&\gamma_6=[120+56E(1+pZ_m)-24M+8K],\\
&\gamma_7=[1+E(1+pZ_m)-M+K+T],\\
&m=0,1,\ldots,N, E=\tfrac{7}{2h}\Delta t, M=\tfrac{42}{h^2}, K=\tfrac{105}{h^3}\Delta t, T=\tfrac{840}{h^4}.
\end{aligned} \quad (2.10)$$

The system (2.9) involves $(N+1)$ linear equations containing $(N+7)$ unknown coefficients $(\delta_{-3},\delta_{-2},\delta_{-1},\ldots,\delta_{N+1},\delta_{N+2},\delta_{N+3})^T$. So, we need six additional restraints to get only a solution for the system. These restraints are got from the Eqs. (1.7) and can be used to remove $\delta_{-3},\delta_{-2},\delta_{-1}$ and $\delta_{N+1},\delta_{N+2},\delta_{N+3}$ from the systems (2.9) which occures a matrix equation contains $N+1$ unknowns $d^n=(\delta_0,\delta_1,\ldots,\delta_N)^T$ of the form

$$R\mathbf{d^{n+1}}=S\mathbf{d^n}. \quad (2.11)$$

The R and S are $(N+1)\times(N+1)$ matrices. A number of inner iterations $\delta^{n*}=\delta^n+\frac{1}{2}(\delta^n-\delta^{n-1})$ are implemented to the terms at each time step to overcome the non-linearity occasioned by Z_m. Before the beginning of the solution procedure, initial parameters d^0 are established by using the initial condition and following derivatives at the boundaries;

$$\begin{aligned}
&U_N(x,0)=U(x_m,0); \qquad m=0,1,2,...,N\\
&(U_N)_x(a,0)=0, \qquad (U_N)_x(b,0)=0,\\
&(U_N)_{xx}(a,0)=0, \qquad (U_N)_{xx}(b,0)=0,\\
&(U_N)_{xxx}(a,0)=0, \qquad (U_N)_{xxx}(b,0)=0.
\end{aligned}$$

Therefore we get the following matrix equation for the initial values of d^0;

$$Vd^0=W,$$

where

$$V=\begin{bmatrix}
1536 & 2712 & 768 & 24 & & & & & & & \\
\frac{82731}{81} & \frac{210568.5}{81} & \frac{104796}{81} & \frac{10063.5}{81} & 1 & & & & & & \\
\frac{9600}{81} & \frac{96597}{81} & \frac{195768}{81} & \frac{96474}{81} & 120 & 1 & & & & & \\
 & & \ddots & & & & & & & & \\
 & & & 1 & 120 & 1191 & 2416 & 1191 & 120 & 1 \\
 & & & & 1 & 120 & \frac{96474}{81} & \frac{195768}{81} & \frac{96597}{81} & \frac{9600}{81} \\
 & & & & & 1 & \frac{10063.5}{81} & \frac{104796}{81} & \frac{210568.5}{81} & \frac{82731}{81} \\
 & & & & & & 24 & 768 & 2712 & 1536
\end{bmatrix}$$

$d^0=(\delta_0,\delta_1,\delta_2,...,\delta_{N-2},\delta_{N-1},\delta_N)^T$ and $W=(U(x_0,0),U(x_1,0),...,U(x_{N-1},0),U(x_N,0))^T$.

3. STABILITY ANALYSIS

To observe the stability analysis of the presented scheme, it is suitable to use Fourier method based on Von-Neumann theory. Presuming that the quantity U^p in the nonlinear term U^pU_x is locally constant. Replacing the Fourier mode $\delta_m^n=\xi^n e^{i\sigma mh}$, $(i=\sqrt{-1})$ into the form of (2.9) we obtain,

$$\begin{aligned}&\xi^{n+1}(\eta_1e^{i(m-3)\theta}+\eta_2e^{i(m-2)\theta}+\eta_3e^{i(m-1)\theta}+\eta_4e^{im\theta}+\eta_5e^{i(m+1)\theta}+\eta_6e^{i(m+2)\theta}+\eta_7e^{i(m+3)\theta})\\&=\xi^n(\eta_7e^{i(m-3)\theta}+\eta_6e^{i(m-2)\theta}+\eta_5e^{i(m-1)\theta}+\eta_4e^{im\theta}+\eta_3e^{i(m+1)\theta}+\eta_2e^{i(m+2)\theta}+\eta_1e^{i(m+3)\theta})\end{aligned}\qquad(3.1)$$

where σ is mode number, h is the element size, $\theta=\sigma h$

$$\begin{aligned}&\eta_1=1-\beta_1-\beta_2-\beta_3+\beta_4,\\&\eta_2=120-56\beta_1-24\beta_2-8\beta_3,\\&\eta_3=1191-245\beta_1-15\beta_2+19\beta_3-9\beta_4,\\&\eta_4=2416+80\beta_2+16\beta_4,\\&\eta_5=1191+245\beta_1-15\beta_2-19\beta_3-9\beta_4,\\&\eta_6=120+56\beta_1-24\beta_2+8\beta_3,\\&\eta_7=1+\beta_1-\beta_2+\beta_3+\beta_4,\\&m=0,1,\ldots,N\quad \beta_1=\tfrac{7\Delta t}{2h}(1+Z_m),\ \beta_2=\tfrac{42}{h^2},\quad \beta_3=\tfrac{105}{h^3}\Delta t,\quad \beta_4=\tfrac{840}{h^4}.\end{aligned}$$

If we simplify the Eq.(3.1),

$$\xi=\frac{A+iB}{A-iB}$$

is obtained where

$$A=(2382-30\beta_2-18\beta_4)\cos(\theta)+(240-48\beta_2)\cos(2\theta)+(2-2\beta_2+2\beta_4)\cos(3\theta)+$$
$$(2416+80\beta_2+16\beta_4),$$
$$B=(490E(1+Z_m)-38\beta_3)\sin(\theta)+(112E(1+Z_m)+16\beta_3)\sin(2\theta)+$$
$$(2E(1+Z_m)+2\beta_3)\sin(3\theta).$$

According to the Fourier stability analysis, for the given scheme to be stable, the condition $|\xi|<1$ must be satisfied. Using a symbolic programming software or using simple calculations, since $a^2+b^2=a^2+(-b)^2$ it becomes evident that the modulus of $|\xi|$ is 1. Therefore our scheme is unconditionally stable.

4. CONVERGENCE OF THE FULL DISCRETE SCHEME

In this study, we approximate the non-linear PDE using special splines for spatial approximations with collocation approach and a one step scheme for time integration. A mater of fact is that the efficiency of a computational algorithm depends on its accuracy and numerical stability. Finite element analysis and approximation is firmly attached in a very elegant framework that enables accurate a priori and a posteriori estimates of convergence rates as well as discretization errors. A large portion of the theory relies on a knowledge of functional analysis which is well developed and discussed in numerous books and articles. Here we study the relevant concepts and key results without proof and cite sources of a more complete treatment. To be specific, we aim for a short discussion about the accuracy of the above mentioned space time scheme without a formal proof. One may consult [12,28,29,30,31] and the references therein for a detailed and settled theories. It is to note that we use some constants $C_i \geq 0$ here which not necessarily the same in all the cases.

Usually global polynomial interpolations are used to integrate the solutions of differential equations for simple computational domain and when unknown curves are considered to be smooth enough. However, most engineering and physical problems are considered when the solutions are not sufficiently smooth to support global polynomial approximation and the computational domain is complicated. For these types of cases finite element approximations play an important role and work very well to represent the solutions of the modelled problem. Polynomial basis functions are smooth which is one of the very important properties in approximation theory. It helps to analyze solutions approximated using the basis functions. Let we have $r+1$ data values. Then there is exactly one polynomial of degree at most r passing through the data points and the error in the interpolating polynomial is proportional to a power of the distance between the data points [29-31]. As stated above we use spetic B-splines along with a collocation approach for the spatial approximation. It is well known that collocation scheme gives super-convergence at collocation points and it does not need an extra inner product to assess as of the Galerkin inner product approach [32]. So this approach is simpler and efficient to calculate solutions.
Let $H^k(\Omega)$ be the space of k times differentiable functions and $\|.\|_r$ be the standard $H^k(\Omega)$ norm. Let v_h be an approximation to a function $v(x)\in H^k(\Omega)$ in Ω . Here $\|.\|_0$ stands for $L_2(\Omega)$ norm. Let h be the distance between the grids and $\Omega=\cup_i\Omega_i$, where $\Omega_i=[x_i,\ x_{i+1}]$, $x_{i+1}=x_i+h$. We notice [30, 31, 33, 34] that

$$\|v(x)-v_h(x)\|\leq Ch^{r+1}\|v\|_{r+1} \ where\, 1\leq r<k,$$

and v_h represents interpolation by piecewise-polynomials of degree r (considering $\Omega = \cup_i \Omega_i$). This error is conserved by the Galerkin finite element approximation as well [12,31]. It is easily seen [12, 29, 34] that if w_h is a proper B-splines identified by a polynomial of degree less or equal k then

$$\left\| w(x) - w_h(x) \right\| \le Ch^{m+1} \left\| w \right\|_{m+1} \; where \, 1 \le m < r,$$

for any $w \in H_r(\Omega)$. For our work we take septic B-splines for space integration. Thus from the above examination one sees that we get a $\mathbf{O}(h^8)$ accuracy for the spatial approximation in $L_2(\Omega)$ norm [12]. For time we choose a forward difference form which is accurate of $\mathbf{O}(\Delta t)$ in $L_2([0\,T])$ norm for some $T > 0$ [31]. So for the space time discretization the error bound is of the form

$$\left\| u(x,t) - u_h(x,t) \right\| \le C_1 h^8 + C_2 \Delta t,$$

for a suitable $C_1 \ge 0$ and $C_2 \ge 0$.

5. NUMERICAL RESULTS AND DISCUSSION

In this part, in order to verify the correction of our numerical algorithm, we consider some experiments involving: the motion of single solitary and shock waves. For these two problems, to see how accurate the numerical algorithm forecasts the position and amplitude of the solution as the simulation proceeds, we use the following error norms:

$$L_2 = \left\| U^{exact} - U_N \right\|_2 = \sqrt{h \sum_{J=0}^{N} \left| U_j^{exact} - \left(U_N\right)_j \right|^2},$$

and

$$L_\infty = \left\| U^{exact} - U_N \right\|_\infty = \max_j \left| U_j^{exact} - \left(U_N\right)_j \right|.$$

There are two conserved quantities for the R-KdV-RLW equation with power law nonlinearity. These are given by

$$\begin{aligned} I_M &= \int_{-\infty}^{\infty} U(x,t)dx, \\ I_E &= \int_{-\infty}^{\infty} [U^2(x,t) - \gamma U_x^2(x,t) + bU_{xx}^2(x,t)]dx \end{aligned} \tag{5.1}$$

which correspond to the momentum and energy of the shallow water waves, respectively [21].

5.1. SOLITARY WAVES

Firstly, Eq. (1.6) is considered with the boundary conditions $U \to 0$ as $x \to \pm\infty$ and the initial condition

$$U(x,0) = A\sec h^{4/n-1}[B(x-x_0)].$$

The exact solution of this problem is found as

$$U(x,t) = A\sec h^{4/n-1}[B(x-vt-x_0)]$$

where A is amplitude of the solitary wave

$$A = [\frac{8(n+1)(n+3)(3n+1)\beta bB^4}{k(n-1)^2[(n-1)^2\gamma + 4(n^2+2n+5)bB^2]}]^{4/n-1},$$

B is inverse width

$$B = \frac{n-1}{n+1}[\frac{D-(n^2+2n+5)ab}{32\beta b}]^{1/2},$$

$$D = \sqrt{a^2b^2(n^2+2n+5)^2 + 16(n+1)^2\beta b(\beta - a\gamma)},$$

v is velocity of the soliton

$$v = [\frac{\beta(n-1)^2}{(n-1)^2\gamma + 4bB^2(n^2+2n+5)}],$$

and x_0 represents the initial center of single solitary wave. The values of the parameters $a=1$, $\gamma=1$, $\beta=1$, $b=1$, $\alpha=1/2$, $n=3$ are taken over the interval $[-40,100]$ to coincide with that of previous papers [18, 26]. Calculations are performed to time $t=30$ to get error norms and two conserved quantities. The obtained datas for different values of h and Δt has been given in Table (5.1.1). Table (5.1.1) shows that invariants are almost constant as time increases. It is noticeably observed from this table that invariants I_M and I_E change from their initial value by less than 1×10^{-5} for different values of h . Also, we have found out error norms L_2 and L_∞ are obtained sufficiently small during the computer run. Therefore we can say our method is sensibly conservative. We compare the values of the error norms derived by our method with methods derived by [18, 26] in Table (5.1.2). This table clearly shows that the error norms obtained by our method are less than the others. Simulations of exact solutions of $U(x,t)$ at $t=0$ and numerical solutions at $t=10,30$ with $h=\Delta t=0.25$ and 0.5 are demonsrated in Figure (5.1.1). We observed from the Figure (5.1.1), the patterns of the numerical solutions are in good agreement with the exact solutions. Also, this figure shows that single soliton travels to the right at a constant speed and conserves its amplitude and shape with increasing time unsurprisingly. Error values between analytical and numerical solutions for $h=\Delta t=0.25$ and 0.5 are shown in Figure (5.1.2), respectively. As it is seen, the maximum errors occur around the central position of the solitary wave.

Table 5.1.1. The invariants and the error norms for single solitary wave for $a=1,\ \gamma=1,\ \beta=1,\ b=1,\alpha=1/2,\ n=3$ over the interval [-40, 100].

$h=\Delta t=0.25$	I_M	I_E	L_2	L_∞
t				
0	21.6792588	43.7172029	0	0
10	21.6683535	43.6837260	9.586739E-02	3.788153E-02
20	21.6575653	43.6506230	1.789812E-01	6.803490E-02
30	21.6468150	43.6176305	2.669906E-01	1.001786E-01
$h=\Delta t=0.125$				
t				
0	21.6792588	43.7172029	0	0
10	21.6778511	43.7128691	2.376454E-02	9.470963E-03
20	21.6764468	43.7085460	4.357827E-02	1.674689E-02
30	21.6750448	43.7042252	6.392907E-02	2.424693E-02
$h=\Delta t=0.0625$				
t				
0	21.6792588	43.7172029	0	0
10	21.6790815	43.7166564	5.895794E-03	2.360596E-03
20	21.6789042	43.7161102	1.069907E-02	4.134279E-03
30	21.6787273	43.7155640	1.553975E-02	5.925496E-03
$h=\Delta t=0.03125$				
t				
0	21.6792588	43.7172029	0	0
10	21.6792366	43.7171345	1.466514E-03	5.885398E-04
20	21.6792144	43.7170660	2.646387E-03	1.025324E-03
30	21.6791923	43.7169976	3.823146E-03	1.462069E-03

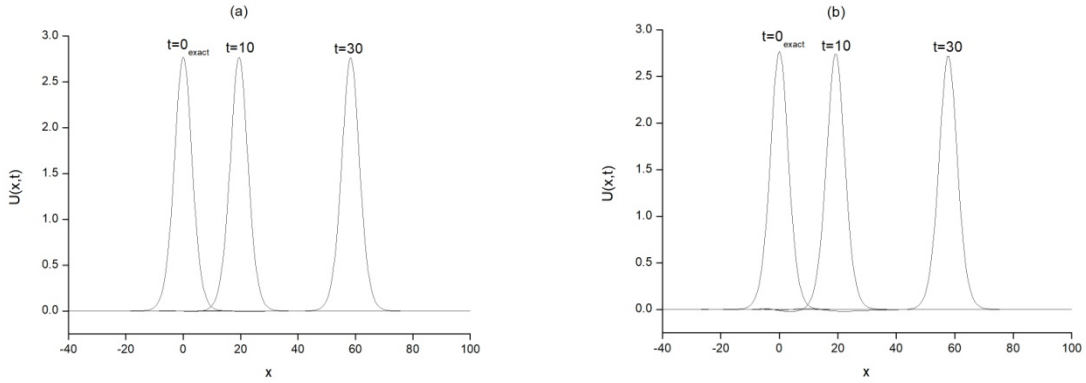

Figure 5.1.1 Motion of single solitary wave for $a=1$, $\gamma=1$, $\beta=1$, $b=1$, $\alpha=1/2$, $n=3$, (a) h =Δt =0. 25, (b) h =Δt =0. 5 over the interval [-40, 100] at specified times.

Table 5.1.2. Comparison of error norms wave for $a=1,\ \gamma=1,\ \beta=1,\ b=1,\ \alpha=1/2,\ n=3$ over the interval [-40, 100] at t=30.

	L_2			L_∞		
	Present	[18]	[26]	Present	[18]	[26]
$h=\Delta t=0.25$	2.66E- 01	5.56E-01	1.86E-00	1.00E-01	2.14E-01	6.99E- 01
$h=\Delta t=0.125$	6.39E- 02	1.34E- 01	5.18E-01	2.42E-02	5.19E- 02	1.97E- 01
$h=\Delta t=0.0625$	1.55E- 02	3.34E- 02	1.33E-01	5.92E-03	1.28E 02	5.06E- 02
$h=\Delta t=0.03125$	3.82E - 03	-	3.35E-02	1.46E-03	-	1.27E- 02

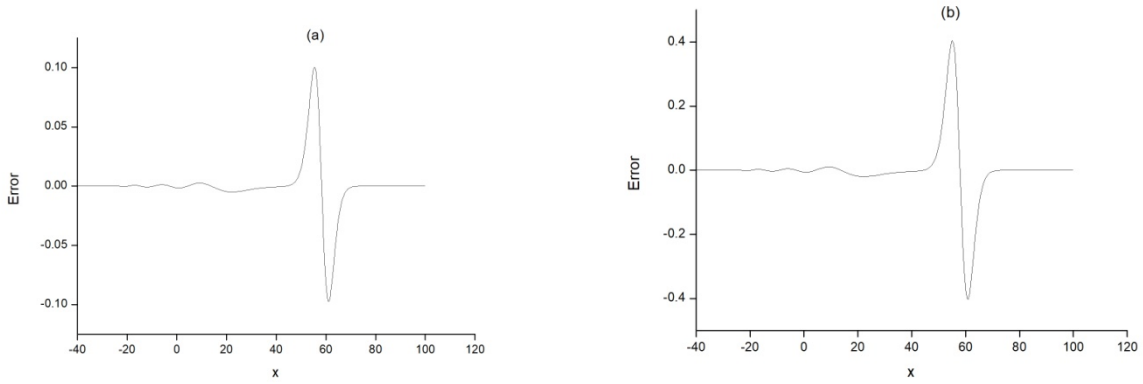

Figure 5.1.2 Errors for $a=1$, $\gamma=1$, $\beta=1$, $b=1$, $\alpha=1/2$, $n=3$, **(a) h =Δt =0. 25, (b) h =Δt =0. 5 at t=40.**

5.2. SHOCK WAVES

In this section, different numerical experiments will be given to illustrate the efficiency and accuracy of the method. For the numerical simulations of the shock wave for which exact solutions have been given before, two sets of parameters are used and discussed. We have found the analytical solution of the problem [21]

$$U(x,t)=A\tanh^{4/n-1}[B(x-vt-x_0)],$$

so the initial condition for this problem is taken as

$$U(x,0)=A\tanh^{4/n-1}[B(x-x_0)]$$

where A is amplitude, B is width and v is velocity of the soliton.

Case 1. For the first numerical calculation, we have considered the problem with parameters $a=1$, $\gamma=0.04$, $\beta=0.025$, $b=1$, $\alpha=1/2$, $n=3$ through the interval $[-200,250]$. For this case,

$$A=2B^2[\frac{30bv}{\alpha}]^{1/2}, v=[\frac{a-8\beta B^2}{136bB^4-8\gamma B^2+1}]$$

and

$$B=[\frac{10ab-\sqrt{100a^2b^2+46\beta b(\beta-a\gamma)}}{92\gamma b}]^{1/2}.$$

Amplitude and velocity of solitary waves are found as $0.00184, v=1.00000$, respectively. The experiment is run from $t=0$ to $t=40$ and values of the error norms are given in Table (5.2.1). Table (5.2.1) indicates that error norms L_2 and L_∞ are sufficiently small during the computer run. Therefore, we clearly say that our numerical method is sensibly conservative. For visual representation, the simulations of single soliton for the values $h=\Delta t=0.1$, 0.2 at times $t=0,10,20,30$ and 40 are illustrated at diverse time levels in Figure (5.2.1). It is understood from this figure that the numerical scheme performs the

motion of propagation of a single solitary wave, which moves to the right at nearly unchanged speed and conserves its amplitude and shape with increasing time. Error distributions with the values of $h = \Delta t = 0.1, 0.2$ at time $t = 40$ are depicted graphically in Figure (5.2.2), respectively. As it is seen, the maximum errors happen around the central position of the solitary wave.

Table 5.2.1. The error norms for shock solitary wave for $a = 1,\ \gamma = 0.04,\ \ \beta = 0.025,\ b = 1,$ $\alpha = 1/2,\ n = 3$ over the interval [-200, 250].

	$h = \Delta t = 0.1$		$h = \Delta t = 0.2$	
t	L_2	L_∞	L_2	L_∞
0	0	0	0	0
10	7.61502E-04	3.21635E-04	8.97653E-04	3.77313E-04
20	1.64258E-03	5.21024E-04	1.89156E-03	5.92167E-04
30	2.56864E-03	6.77248E-04	2.90744E-03	7.53014E-04
40	3.52276E-03	8.10797E-04	3.93320E-03	8.87275E-04

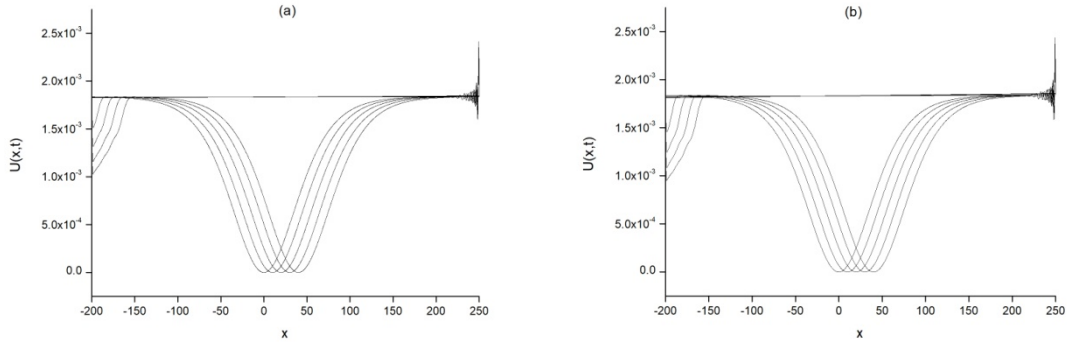

Figure 5.2.1. Shock wave with amplitude $A = 0.00184,\ v = 1.00000,\ a = 1,\ \gamma = 0.04\ \ \beta = 0.025,$ $b = 1,\ \alpha = 5,\ n = 3,$ (a) h =Δt =0. 1, (b) h =Δt =0. 2 over the interval [-200, 250] at specified times.

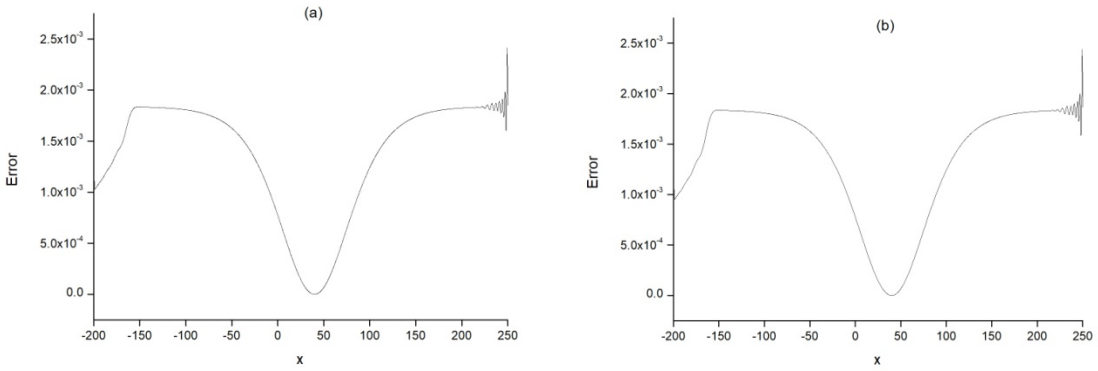

Figure 5.2.2. Errors for shock wave with amplitude $A = 0.00184,\ v = 1.00000,\ a = 1,\ \gamma = 0.04$ $\beta = 0.025,\ b = 1,\ \alpha = 5,\ n = 3,$ (a) h =Δt =0. 1, (b) h =Δt =0. 2 over the interval [-200, 250] at t=40.

Case 2. For the second numerical calculation, we have used the parameter $n=5$ with values of $h=\Delta t=0.05$ and 0.1 through the interval $[-100,100]$. For this case,

$$A=B[\frac{24bv}{\alpha}]^{1/4}, v=[\frac{a-2\beta B^2}{16bB^4-2\gamma B^2+1}]$$

and

$$B=[\frac{5ab-\sqrt{25a^2b^2+6\beta b(\beta-a\gamma)}}{12\gamma b}]^{1/2}.$$

Amplitude and velocity of solitary waves are found as 0.02641, $v=0.12500$, respectively. The run of the algorithm is carried up to time $t=40$ to obtain error norms at various times. The obtained results are tabulated in Table (5.2.2). It is noticeably seen from the table that the error norms L_2 and L_∞ are obtained enough small during the computer run. The behaviours of solutions for values $h=\Delta t=0.1$, 0.05 at times $t=0,10,20,30$ and 40 have been shown in Figure (5.2.3). From this figure, we can see that the solitary wave moves to the right at constant velocity and remains its shape and amplitude. The error graph at $t=40$ is given in Figure (5.2.4). It is observed that the maximum errors are about the tip of the solitary waves and between -5×10^{-4} and - 3.5×10^{-3}.

Table 5.2.2. The error norms for shock solitary wave for $a=0.125$, $\gamma=0.5$, $\beta=0.04$, $b=20$, $\alpha=25$, $n=5$ over the interval [-100; 100].

	$h=\Delta t=0.1$		$h=\Delta t=0.05$	
t	L_2	L_∞	L_2	L_∞
0	0	0	0	0
10	2.15972E-03	8.34524E-04	2.19797E-03	8.50263E-04
20	4.32163E-03	1.63917E-03	4.39753E-03	1.67045E-03
30	6.50620E-03	2.41090E-03	6.61959E-03	2.45838E-03
40	8.73147E-03	3.19204E-03	8.88257E-03	3.24193E-03

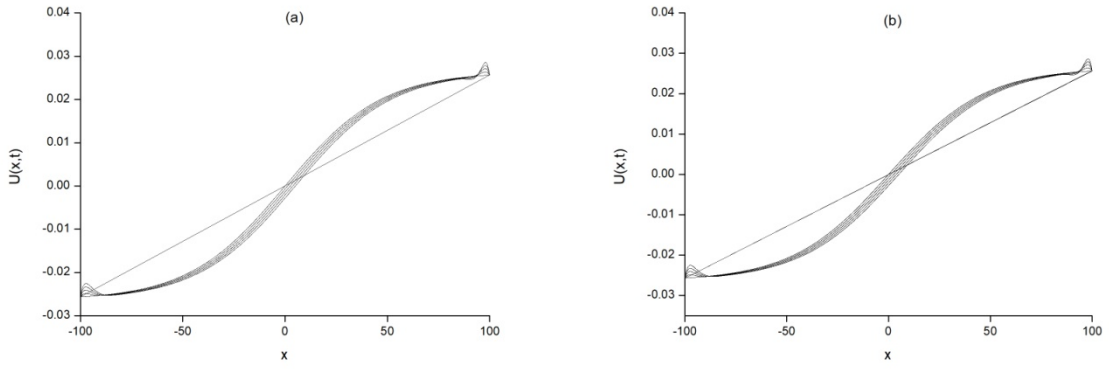

Figure 5.2.3. Shock wave with amplitude $A=0.02641$, $v=0.12500$, $a=0.125$, $\gamma=0.5$ $\beta=0.04$, $b=1$, $\alpha=25$, $n=5$, (a) h =Δt =0. 1, (b) h =Δt =0. 05 over the interval [-100, 100] at specified times.

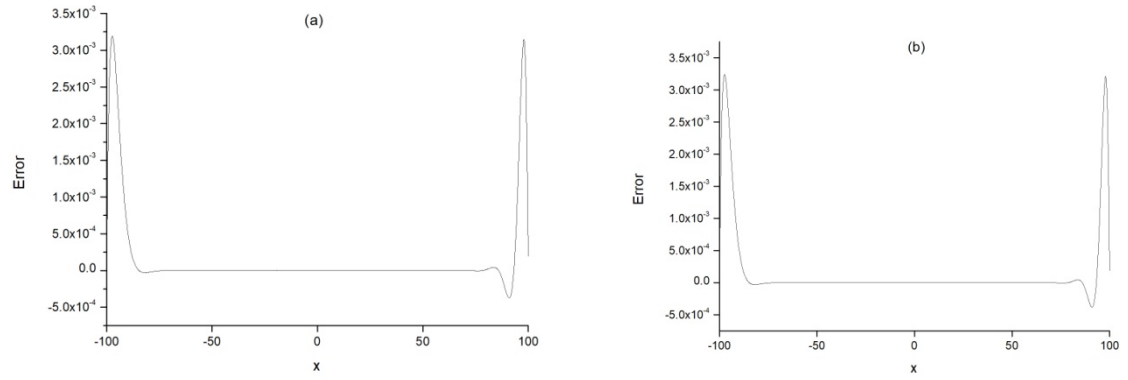

Figure 5.2.4. Errors for shock wave with amplitude $A = 0.02641$, $v = 0.12500$, $a = 0.125$, $\gamma = 0.5$ $\beta = 0.04$, $b = 1$, $\alpha = 25$, $n = 5$, **(a) h =Δt =0. 1, (b) h =Δt =0. 05 over the interval [-100, 100] at t=40.**

6. CONCLUSION

In this study, a septic B-spline collocation method has been proposed and successfully applied to the R-KdV-RLW equation to examine the motion of a single solitary and shock waves whose analytical solutions are known. To investigate the efficiency and accuracy of the numerical solutions of the test problems, we have computed the error norms L_2 and L_∞ and conserved quantities I_M and I_E. The illustrative numerical results indicate that the error norms are satisfactorily small and the conservation laws are marginally constant. It is well observed that the proposed scheme is more accurate than the other earlier schemes found in the literature. We have also analyzed the numerical stability of the scheme. It is established that the linearized numerical scheme is unconditionally stable. Therefore, we conclude that the proposed numerical scheme is useful and efficient to obtain the numerical solutions of other important nonlinear problems in various fields.

Acknowledgment: *Fuzheng Gao's research is supported in part by China Postdoctoral Science Foundation no. 2014M560547, Fundamental Research Funds of Shandong University no. 2017JC005 and National Natural Science Foundation of China (NSFC) no. 11771367.*

REFERENCE

[1] Peregrine, D.H., *J. Fluid Mech.*, **25**, 321, 1996.
[2] Korteweg, D.J., de Vries, G., *Philosophical Magazine*, **39**, 422, 1895.
[3] Pan, X., Zhang, L., *Applied Mathematics and Computation*, **218**, 8917, 2012.
[4] Rosenau, P., *Phys. Scripta*, **34**, 827, 1986.
[5] Rosenau, P., *Progr. Theory. Phys.*, **79**, 1028, 1988.
[6] Park, M.A., *Math. Appl. Comput.*, **9,** 145, 1990.
[7] Zuo, J.M., *Applied Mathematics and Computation.*, **215**, 835, 2009.
[8] Hu, J., Xu, Y., Hu, B., *Advances in Mathematical Physics*, **2013**, Article ID 423718, 2013.

[9] Ebadi, G., Mojaver, A., Triki, H., Yildirim, A., Biswas, A., *Rom. J. Physics*, **58**(1-2), 3, 2013.
[10] Razborova, P., Triki, H., Biswas, A., *Ocean Engineering*, **63**, 1, 2013.
[11] Ak, T., Karakoc, S.B.G., Triki, H., *Eur. Phys. J. Plus*, **131**, 356, 2016.
[12] Ak, T., Dhawan, S., Karakoc, S.B.G., Bhowmik, S.K., Raslan, K.R., *Mathematical Modelling and Analysis*, **22**(3), 373, 2017.
[13] Pan, X., Zhang, L., *Appl. Math. Model*, **36**, 3371, 2012.
[14] Pan, X., Zheng, K., Zhang, L., *Appl. Anal*, **92**, 2578, 2013.
[15] Zuo, J., Zhang, Y.M., Zhang, T. D., Chang, F., *Bound. Value Probl*, **2010**, 1, 2010.
[16] Atouani, N., Omrani, K., *Computers and Mathematics with Applications*, **66**, 289, 2013.
[17] Yagmurlu, N.M., Karaagac, B., Kutluay, S., *American Journal of Computational and Applied Mathematics*, **7**(1), 1, 2017.
[18] Wongsaijai, B.,Poochinapan, K., *Applied Mathematics and Computation*, **245**, 289, 2014.
[19] Razborova, P., Moraru, L., Biswas, A., *Romanian Journal of Physics*, **59** (7-8), 658, 2014.
[20] Razborova, P., Kara, Abdul H., Biswas, A., *Nonlinear Dynamics*, **79**(1):743, 2014.
[21] Razborova, P., Ahmed, B., Biswas, A., *Appl.Math. Inf. Sci*., **8**(2), 485, 2014.
[22] Cai, J., Liang, H., Zhang, C., *Commun. Nonlinear Sci. Numer. Simulat*., **59**, 122, 2018.
[23] Cai, J., Hong, Q., Yang, B., *Chin. Phys. B*, **26**(10) 2017.
[24] Ak, T., Karakoc, S.B.G., Biswas, A., *Journal of Comput. and Theor. Nanoscience*, **13**, 7084, 2016.
[25] Apolinar-Fernández, A., Ramos, J.I., *Commun. Nonlinear Sci. Numer. Simulat*., **60**, 165, 2018.
[26] Wang, X., Dai, W., *Journal of Computational and Applied Mathematics*, **330**, 295, 2018.
[27] Prenter, P.M., *Splines and Variational Methods*. John Wiley & Sons, New York, 1975.
[28] Bhowmik, S.K., Belbakib, R., Boulmezaoudc, T.Z., Mziou, S., *Computers & Mathematics with Applications*, **67**(10), 2027, 2014.
[29] Bochev, P.B., Gunzburger, M.D., *Least-Squares Finite Element Methods*, Springer, 2008.
[30] Suli, A., Mayers, D., *An Introduction to Numerical Analysis*, Cambridge University Press, 2003.
[31] Thomee, V., *Galerkin Finite Element Methods for Parabolic Problems*, Second edition, Springer, 2006.
[32] Gomez, H., De Lorenzis, L., *Computer Methods in Applied Mechanics and Engineering*, **309**, 152, 2016.
[33] Bhowmik, S.K., *Mathematical Analysis and Applications*, 420(2), 1069, 2014.
[34] Dhawan, S., Bhowmik, S.K., Kumar, S., *Applied Mathematics and Computation*, **261**, 128, 2015.